

Self-avoiding polygons and walks in slits

J Alvarez^{1,2}, E J Janse van Rensburg², C E Soteros³ and S G Whittington¹

¹ Department of Chemistry, University of Toronto, Toronto, ON M5S 3H6, Canada

² Department of Mathematics and Statistics, York University, Toronto, ON M3J 1P3, Canada

³ Department of Mathematics and Statistics, University of Saskatchewan, Saskatoon, SK S7N 5E6, Canada

E-mail: jalvarez@chem.utoronto.ca, rensburg@yorku.ca, soteros@math.usask.ca and swhittin@chem.utoronto.ca

Received 12 February 2008, in final form 27 March 2008

Published 18 April 2008

Online at stacks.iop.org/JPhysA/41/185004

Abstract

A polymer in a confined geometry may be modeled by a self-avoiding walk or a self-avoiding polygon confined between two parallel walls. In two dimensions, this model involves self-avoiding walks or self-avoiding polygons in the square lattice between two parallel confining lines. Interactions of the polymer with the confining walls are introduced by energy terms associated with edges in the walk or polygon which are at or near the confining lines. We use transfer-matrix methods to investigate the forces between the walk or polygon and the confining lines, as well as to investigate the effects of the confining slit's width and of the energy terms on the thermodynamic properties of the walks or polygons in several models. The phase diagram found for the self-avoiding walk models is qualitatively similar to the phase diagram of a directed walk model confined between two parallel lines, as was previously conjectured. However, the phase diagram of one of our polygon models is found to be significantly different and we present numerical data to support this. For that particular model we prove that, for any finite values of the energy terms, there are an infinite number of slit widths where a polygon will induce a steric repulsion between the confining lines.

PACS numbers: 05.50.+q, 82.35.Lr, 82.35.Gh, 61.25.Hq

(Some figures in this article are in colour only in the electronic version)

1. Introduction

Models of polymers confined between two parallel walls have been studied partly because of an interest in the effect of geometrical constraints on the configurational and thermodynamic properties of polymers and partly as models of steric stabilization and sensitized flocculation

[1]. When a polymer is confined between two parallel walls the polymer loses configurational entropy and this results in a repulsive force being exerted by the polymer on the confining walls. When the polymer adsorbs on the two attractive confining walls the resulting attractive force can dominate the entropic repulsion.

In a classic paper DiMarzio and Rubin [2] investigated a random walk model of a polymer between two parallel walls in the cubic lattice. Interactions between the walk and the wall, besides the geometric constraints, were modeled through energy terms in the Boltzmann weights of the walks. If the energy terms are not present then the confined walk loses entropy and the force exerted by the walk on the walls is always repulsive. If the walk is attracted to only one of the two walls the force remains repulsive. However, if the walk is attracted (equally) to both walls then the force is repulsive for weak attractive interactions but the force is attractive for stronger attractive interactions—see for example [1, 3–5] for more remarks and results.

In 2005, Brak *et al* [6] considered a two-dimensional directed walk version of this model. They considered a Dyck path confined between the two lines $y = 0$ and $y = w$, where vertices of the Dyck path are given a Boltzmann weight a if they are in the line $y = 0$ and a weight b if they are in the line $y = w$. For an infinite Dyck path (that is, a Dyck path with n edges where $n \rightarrow \infty$) they investigated the behavior at large but finite w as a function of a and b . In this model they showed that there is a zero-force curve ($ab = a + b$) separating the region where the force is repulsive from where it is attractive. In the attractive regime the force is always short-ranged but in the repulsive regime there are regions where the force is long-ranged and regions where it is short-ranged. The behavior when n and w are both finite has recently been investigated by Owczarek *et al* [7]. The results for Dyck paths (in the infinite n limit) were extended to Motzkin paths by Brak *et al* [8], and the phase diagram is qualitatively similar to that found for Dyck paths.

Self-avoiding walks confined between two parallel walls with Boltzmann weights $a = b = 1$ have also been considered. Wall *et al* [9] studied the mean square end-to-end separation of self-avoiding walks on the square lattice between two parallel lines and obtained exact results for a slit of width $w = 1$ as well as asymptotic results for a slit of width $w = 2$. Wall and coworkers [10, 11] used Monte Carlo methods to study the problem and calculated the exponential growth rate of self-avoiding walks on the square lattice between two parallel lines for small w . These calculations were extended by Klein [12] and by Alm and Janson [13]. Hammersley and Whittington [14] showed that the force was repulsive for all values of w .

More recently, Janse van Rensburg *et al* [4] generalized the results of Hammersley and Whittington to include interactions with the confining planes besides the geometric constraints and showed that the force is repulsive in certain regions of the (a, b) -plane. Although there are numerical results which suggest that the phase diagram for self-avoiding walks is qualitatively similar to that of directed walks (such as Dyck and Motzkin paths) there are no rigorous results establishing the existence of an attractive force for some values of a and b .

In this paper we consider both self-avoiding walks and self-avoiding polygons on the square lattice confined between the two lines $y = 0$ (bottom wall) and $y = w$ (top wall).

Let \vec{v} be the non-negative integer vector $(v_0, v_{0,1}, v_1, v_{w-1}, v_{w-1,w}, v_w)$ and let $c_n(\vec{v}, w)$ be the number of self-avoiding walks in a slit of width w with n edges, having v_0 horizontal edges at $y = 0$ (the bottom wall), v_1 horizontal edges at $y = 1$ (immediately above the bottom wall), $v_{0,1}$ vertical edges between $y = 0$ and $y = 1$ (to/from the bottom wall), v_w horizontal edges at $y = w$ (the top wall), v_{w-1} horizontal edges at $y = w - 1$ (immediately below the top wall), and $v_{w-1,w}$ vertical edges between $y = w - 1$ and $y = w$ (to/from the top wall).

One can define the partition function as

$$Z_n(\vec{a}, \vec{b}, w) = \sum_{\vec{v}} c_n(\vec{v}, w) a_0^{v_0} a_{0,1}^{v_{0,1}} a_1^{v_1} b_{t-1}^{v_{t-1}} b_{t-1,t}^{v_{t-1,t}} b_t^{v_t}, \quad (1)$$

where \vec{a} is the positive real vector of Boltzmann factors $(a_0, a_{0,1}, a_1)$ and \vec{b} is the positive real vector of Boltzmann factors $(b_{t-1}, b_{t-1,t}, b_t)$. We shall refer to the Boltzmann factors as *wall interaction parameters*. The grand canonical partition function is given by

$$H(\vec{a}, \vec{b}, w, z) = \sum_{n=0}^{\infty} Z_n(\vec{a}, \vec{b}, w) z^n \quad (2)$$

whose radius of convergence, $z_c(H(\vec{a}, \vec{b}, w, z))$, is positive and finite. The radius of convergence is positive because all terms in the grand canonical partition function are positive, and it will be shown to be finite in section 3.

The free energy is defined in terms of the partition function (1) as

$$\kappa(\vec{a}, \vec{b}, w) = \lim_{n \rightarrow \infty} n^{-1} \log Z_n(\vec{a}, \vec{b}, w), \quad (3)$$

where the existence of the limit follows *mutatis mutandis* from [4]. The free energy may also be obtained from the radius of convergence $z_c(H(\vec{a}, \vec{b}, w, z))$ as:

$$\kappa(\vec{a}, \vec{b}, w) = -\log(z_c(H(\vec{a}, \vec{b}, w, z))). \quad (4)$$

The force exerted by the walk (or the polygon) on the confining lines is defined as

$$f(\vec{a}, \vec{b}, w) := \frac{\partial}{\partial w} \kappa(\vec{a}, \vec{b}, w) \approx \kappa(\vec{a}, \vec{b}, w + 1) - \kappa(\vec{a}, \vec{b}, w), \quad (5)$$

where we approximate the derivative by a difference relation because in this paper we obtain the free energy $\kappa(\vec{a}, \vec{b}, w)$ only for integer width values w . If the free energy increases as the width w increases, then the force is positive and hence it is a repulsive force. On the other hand, if the free energy decreases as the width w increases, then the force is negative and hence it is an attractive force.

We consider four special cases of the partition function (1):

- (1) $a_{0,1} = a_1 = b_{t-1} = b_{t-1,t} = 1$, which we shall refer to as the model with *single layers at both walls* (section 4.1),
- (2) $a_{0,1} = a_1 = b_{t-1,t} = 1$ and $b_{t-1} = b_t = b$, which we shall refer to as the model with a *double layer at the top wall* (section 4.2),
- (3) $a_{0,1} = b_{t-1,t} = 1$, $a_0 = a_1 = a$ and $b_{t-1} = b_t = b$, which we shall refer to as the model with *double layers at both walls* (section 4.3),
- (4) $a_0 = a_{0,1} = a_1 = a$ and $b_{t-1} = b_{t-1,t} = b_t = b$, which we shall refer to as the model with *fully interacting double layers* (section 4.4).

We are interested in the behavior of the walk (or the polygon) as a function of the wall interaction parameters \vec{a} and \vec{b} and of the width w . In particular, are there both attractive and repulsive regimes in the phase diagram, and if so, how are they arranged? The phase diagram for directed walk models was investigated in the large- w regime [6, 8] and several different force regimes were identified: a long-ranged and repulsive regime, a short-ranged and attractive regime, and a short-ranged and repulsive regime.

In this paper we examine the phase diagram of the four models described above by transfer-matrix methods (for a discussion of transfer matrices, see for example [15, section 4.7]). Our implementation will follow the methods discussed in [3, 12]. In section 2 we describe a representation of self-avoiding walks and self-avoiding polygons as sequences

of column states, as described in [12]. The application of the transfer-matrix method to our models is discussed in section 3 for both self-avoiding walks and self-avoiding polygons.

In section 4 we present our numerical results. In the model with single layers at both walls we find qualitatively different behavior for the walk and the polygon models. In the walk model we find both repulsive and attractive regimes in the ab -plane separated by a zero-force curve. This zero-force curve is asymptotic to the lines $a = 1$ and $b = 1$ in this model. In the polygon model there is no evidence of an attractive phase, presumably because the polygon screens itself in a two-dimensional slit. We prove that for infinitely many values of the slit width w , there is no attractive regime in the polygon model with single layers at both walls. However, we have not ruled out the existence of attractive forces for some values of w .

The other models have not been previously considered. Our results show the presence of an attractive regime in all these models, in contrast to the polygon model with single layers at both walls. We conclude the paper with final remarks in section 5.

2. Column state representation

Klein [12] described how to represent a two-dimensional unfolded self-avoiding walk in a slit as a sequence of *column states*, as will be described in section 2.1. This representation is similarly applicable to two-dimensional self-avoiding polygons in a slit, as discussed in section 2.2. This column state representation allows the application of transfer-matrix methods to study the behavior of the walk or the polygon, as will be discussed in section 3.

2.1. Self-avoiding walks

The discussion here is limited to *unfolded walks* in the square lattice. An unfolded walk $\omega = \{\omega_0, \omega_1, \dots, \omega_n\}$ of length n and with vertices ω_i with coordinates $(x(\omega_i), y(\omega_i))$ satisfies the constraint $x(\omega_0) < x(\omega_i) < x(\omega_n)$ for $i = 1, 2, \dots, n$. In other words, the first vertex is strictly ‘left-most’ (has least x -coordinate), and the last vertex is strictly ‘right-most’ (has maximal x -coordinate). Unfolded walks were introduced in [16] and it can be proven using the methods of [4] that unfolded walks with the partition function given by (1) have the same limiting free energy as all walks.

Following Klein [12], an unfolded two-dimensional self-avoiding walk in a slit of width w may be considered as a sequence of *column states*, where the i th column state corresponds to the i th column of horizontal edges combined with a specification of how these edges are connected through previous column states. This allows walks to be constructed from a sequence of column states while tracking the connectivity and self-avoidance of the walk as the states are appended on the right. For example, consider a slit of width $w = 1$, then there are only two possible column states, S_1 and S_2 , for unfolded self-avoiding walks, as depicted in figure 1(a). Figure 1(b) depicts an example of the column state representation for a particular self-avoiding walk of length $n = 11$ consisting of the sequence of 8 column states $(S_1, S_1, S_2, S_2, S_2, S_2, S_1, S_2)$. In the slit of width $w = 1$, one can go from any column state to any other column state, with the possible addition of a vertical edge to connect the horizontal edges in adjacent column states (e.g., to connect the second and third columns of the self-avoiding walk in figure 1).

Figure 2(a) shows the five possible column states, S_1, \dots, S_5 , for unfolded self-avoiding walks in a slit of width $w = 2$. The rounded vertical edges in the column states S_4 and S_5 specify how the corresponding horizontal edges must be connected through previous column states. In particular, if a walk is generated from a sequence of column states, then there is

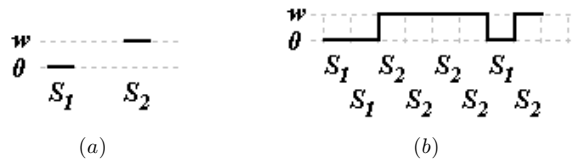


Figure 1. (a) Possible column states, S_1 and S_2 , for unfolded self-avoiding walks in a slit of width $w = 1$. (b) An example of the column state representation of a self-avoiding walk of length $n = 11$ consisting of the sequence of 8 column states $(S_1, S_1, S_2, S_2, S_2, S_2, S_1, S_2)$.

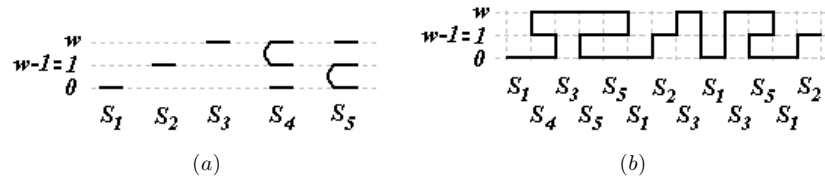


Figure 2. (a) Possible column states, S_1, \dots, S_5 , for unfolded self-avoiding walks in a slit of width $w = 2$. (b) An example of the column state representation of a self-avoiding walk of length $n = 34$ consisting of 13 columns. This self-avoiding walk can be represented as the sequence of column states $(S_1, S_4, S_3, S_5, S_5, S_1, S_2, S_3, S_1, S_3, S_5, S_1, S_2)$.

a set of matching rules which gives, for each column state, the possible states to which it may be appended on the right by the addition of vertical edges. For example, one may not append column states S_5 to S_1 on the right because there is no possible selection of vertical edges which would give a consistent self-avoiding matching of these two states. Figure 2(b) depicts an example of the column state representation of a particular self-avoiding walk of length $n = 34$ consisting of the sequence of 13 column states $(S_1, S_4, S_3, S_5, S_5, S_1, S_2, S_3, S_1, S_3, S_5, S_1, S_2)$.

In order to calculate the number of possible column states for unfolded self-avoiding walks in a slit of width w , one has to take into account the number and location of the horizontal edges in the column state as well as the specification for how they are connected to one another by previous column states. First note that each column state must have an odd number of horizontal edges. So, for a slit of width w , one can have column states with $1, 3, \dots, 2\lfloor w/2\rfloor + 1$ horizontal edges. Then, one may have column states with the same number of horizontal edges but with their horizontal edges having different sets of y -coordinates. If the slit has width w , then there are $\binom{w+1}{2m+1}$ different choices for the y -coordinates of $2m + 1$ horizontal edges. Finally, given a set of $2m + 1$ horizontal edges, we must consider how many ways there are to specify how these edges should be connected through previous column states. If there are $2m + 1$ horizontal edges in a particular column state, then $2m$ of them must be connected in pairs through previous column states without their paths crossing one another (otherwise the self-avoidance constraint is violated). The remaining edge must then be able to be extended indefinitely to the left without crossing any of the paths between the other $2m$ horizontal edges. This infinite extension is equivalent to requiring that the remaining edge be connected on the left to an additional horizontal edge below the lowest edge (or above the highest edge). With the addition of a horizontal edge at height $y = -1$, a specification of how the original $2m + 1$ horizontal edges can be connected is thus equivalent to a pairing of the now $2m + 2$ horizontal

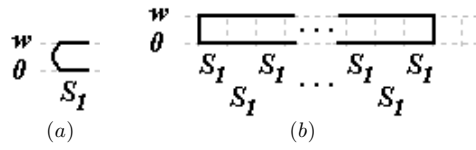


Figure 3. (a) Possible column states for self-avoiding polygons in a slit of width $w = 1$. (b) An example of the column state representation of a self-avoiding polygon.

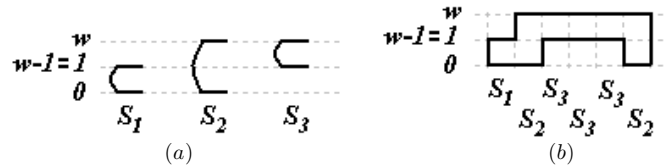


Figure 4. (a) Possible column states, S_1, S_2, S_3 , for self-avoiding polygons in a slit of width $w = 2$. (b) An example of the column state representation of a self-avoiding polygon of length $n = 18$ consisting of the sequence of 6 column states $(S_1, S_2, S_3, S_3, S_3, S_2)$.

edges; the edges must be paired up using a set of $m + 1$ non-intersecting lines (on the left) that join the left-most end points of a paired set of horizontal edges. This problem is then equivalent to calculating the number of ways of joining $2m + 2$ points on a circle to form $m + 1$ non-intersecting chords. This can be done in C_{m+1} ways, where C_m is the m th Catalan number [17] given by $\frac{1}{m+1} \binom{2m}{m}$. Thus, the number of possible column states for unfolded self-avoiding walks in a slit of width w , denoted by c_w , is given by [12]:

$$\begin{aligned}
 c_w &= \sum_{m=0}^{\lfloor w/2 \rfloor} \binom{w+1}{2m+1} C_{m+1} = \sum_{m=0}^{\lfloor w/2 \rfloor} \frac{2(w+1)!}{(w-2m)!m!(m+2)!} \\
 &= (w+1) {}_2F_1 \left(\frac{-w}{2}, \frac{-w+1}{2}, 3, 4 \right), \tag{6}
 \end{aligned}$$

where ${}_2F_1(x_1, x_2, y_1, z)$ is the hypergeometric function. The first few values of c_w for widths $w = 1, \dots, 20$ are 2, 5, 12, 30, 76, 196, 512, 1353, 3610, 9713, 26324, 71799, 196938, 542895, 1503312, 4179603, 11662902, 32652735, 91695540, 258215664.

2.2. Self-avoiding polygons

Similarly, a two-dimensional self-avoiding polygon in a slit of width w can be considered as a sequence of column states. In a slit of width $w = 1$, there is only one possible column state, S_1 , for self-avoiding polygons as depicted in figure 3(a). The self-avoiding polygon in figure 3(b) can be represented as the sequence of column states $(S_1, S_1, S_1, \dots, S_1, S_1, S_1)$.

Figure 4(a) shows the three possible column states, S_1, S_2, S_3 , for self-avoiding polygons in a slit of width $w = 2$. If a polygon is generated from a sequence of column states, then there is again a set of matching rules which gives, for each column state, the possible states to which it may be appended on the right by the addition of vertical edges. For example, one may not append column state S_1 to S_3 on the right because there is no possible selection of vertical

edges which would give a consistent self-avoiding matching of these two states. Figure 4(b) depicts an example of the column state representation for a particular self-avoiding polygon of length $n = 18$ consisting of the sequence of 6 column states $(S_1, S_2, S_3, S_3, S_3, S_2)$.

Following an argument similar to that given in section 2.1 for self-avoiding walks, the number of possible column states for self-avoiding polygons in a slit of width w , denoted by \hat{c}_w , is given by [12]:

$$\begin{aligned} \hat{c}_w &= \sum_{m=1}^{\lfloor (w+1)/2 \rfloor} \binom{w+1}{2m} C_m = \sum_{m=1}^{\lfloor (w+1)/2 \rfloor} \frac{(w+1)!}{(w+1-2m)!m!(m+1)!} \\ &= \frac{w(w+1)}{2} {}_3F_2 \left(1, \frac{-w+2}{2}, \frac{-w+1}{2}, 2, 3, 4 \right), \end{aligned} \tag{7}$$

where ${}_pF_q(x_1, \dots, x_p, y_1, \dots, y_q, z)$ is the generalized hypergeometric function with p parameters of type 1 and q parameters of type 2. The first few values of \hat{c}_w for widths $w = 1, \dots, 20$ are 1, 3, 8, 20, 50, 126, 322, 834, 2187, 5797, 15 510, 41 834, 113 633, 310 571, 853 466, 2356 778, 6536 381, 18 199 283, 50 852 018, 142 547 558.

3. Transfer-matrix setup

Given a fixed positive integer width w and a fixed positive integer number of columns c , one can count (up to equivalency under horizontal translation) the number of unfolded self-avoiding walks in a slit of width w with c columns by means of a transfer-matrix [3, 12]. Furthermore, the transfer matrix can be used to weight each of these self-avoiding walks according to any parameters that depend only on individual column states and pairs of consecutive column states. For example, one may choose to weight according to the number of edges, the number of edges at each height y (in particular, at the top and bottom confining lines), etc. The remainder of this section will consider the self-avoiding walk case, but a weighted count of self-avoiding polygons can be treated in a similar manner.

For a fixed width w let M be a $c_w \times c_w$ matrix, where c_w is the number of possible column states, given by (6). The entry in the i th row and j th column of M , denoted by m_{ij} , is zero if column state j cannot follow column state i in the construction of a self-avoiding walk. Otherwise, we first suppose that we are building a self-avoiding walk column-state-by-column-state and currently the walk ends at column state i . Suppose next that the walk is extended by appending column state j on the right, then m_{ij} is equal to the factor that is contributed to the weight of the walk due to the addition of column state j . In accordance with the grand canonical partition function (2), m_{ij} has a factor

- a_0 if column state j has a horizontal edge at $y = 0$ (the bottom wall),
- a_1 if it has a horizontal edge at $y = 1$ (immediately above the bottom wall),
- $a_{0,1}$ if a vertical edge is needed between $y = 0$ and $y = 1$ to keep connectivity when column state j is appended to column state i on the right,
- b_t if column state j has a horizontal edge at $y = w$ (the top wall),
- b_{t-1} if it has a horizontal edge at $y = w - 1$ (immediately below the top wall),
- $b_{t-1,t}$ if a vertical edge is needed between $y = w - 1$ and $y = w$ to keep connectivity when column state j is appended to column state i on the right, and
- z for each edge, either vertical or horizontal, arising from appending column state j to column state i on the right.

For example, consider the slit of width $w = 2$, then the matrix M is given by

$$M = \begin{pmatrix} z a_0 & z^2 a_1 a_{0,1} & z^3 a_{0,1} b_{t-1,t} b_t & z^4 a_0 a_1 b_{t-1} b_{t-1,t} b_t & 0 \\ z^2 a_0 a_{0,1} & z a_1 b_{t-1} & z^2 b_{t-1,t} b_t & 0 & 0 \\ z^3 a_0 a_{0,1} b_{t-1,t} & z^2 a_1 b_{t-1,t} b_{t-1} & z b_t & 0 & z^4 a_0 a_{0,1} a_1 b_{t-1} b_t \\ 0 & 0 & z^2 b_t & z^3 a_0 a_1 b_{t-1} b_t & 0 \\ z a_0 & 0 & 0 & 0 & z^3 a_0 a_1 b_{t-1} b_t \end{pmatrix} \quad (8)$$

where the column states are labeled as in figure 2.

The matrix M for self-avoiding polygons in a slit of width w is constructed in the same manner. As an example, we present the matrix M for self-avoiding polygons in a slit of width $w = 2$:

$$M = \begin{pmatrix} z^2 a_0 a_1 b_{t-1} b_t & z^3 a_0 b_{t-1,t} b_t & 0 \\ z^3 a_0 a_1 b_{t-1} b_{t-1,t} & z^2 a_0 b_t & z^3 a_{0,1} a_1 b_{t-1} b_t \\ 0 & z^3 a_0 a_{0,1} b_t & z^2 a_1 b_{t-1} b_t \end{pmatrix} \quad (9)$$

where the column states are labeled as in figure 4.

As described by Stilck and Machado [3], one can then define for each column state $c = 1, \dots, c_w$ a partial partition function

$$g_x(c) = \sum_{n, \vec{v}_{x,c}} c_n(\vec{v}_{x,c}, w) a_0^{v_0} a_1^{v_1} a_{0,1}^{v_{0,1}} b_t^{v_w} b_{t-1}^{v_{w-1}} b_{t-1,t}^{v_{w-1,w}} z^n, \quad (10)$$

where $c_n(\vec{v}_{x,c}, w)$ is the number of self-avoiding walks with the following three properties: they start with one of the $w + 1$ column states that have a single horizontal edge, they consist of a sequence of x column states and, their last column is in column state c . Then, by appending any column state \hat{c} on the right one can obtain the following recursion relation for the $g_x(c)$'s:

$$g_{x+1}(\hat{c}) = \sum_{c=1}^{c_w} g_x(c) m_{c\hat{c}}. \quad (11)$$

The fact that we are considering unfolded self-avoiding walks yields the initial conditions

$$g_0(c) = \sum_{\hat{c}=1}^{w+1} \delta_{c,\hat{c}} \quad (12)$$

where the convention is made to label the column states in such a way that the first $w + 1$ of them consist of a single horizontal edge.

Then, the grand canonical partition function for all unfolded self-avoiding walks ending with column state c can be defined as

$$G(c) = \sum_{x=0}^{\infty} g_x(c). \quad (13)$$

Based on the recursion relations (11), these grand canonical partition functions satisfy a set of c_w linear equations

$$\sum_{c=1}^{c_w} G(c) (m_{c\hat{c}} - \delta_{\hat{c},c}) = -g_0(\hat{c}). \quad (14)$$

This set of linear equations can be written in a matrix form as

$$\vec{G}(M - I) = -\vec{g}_0, \quad (15)$$

where $\vec{G} = (G(1), \dots, G(c_w))$ and $\vec{g}_0 = (g_0(1), \dots, g_0(c_w))$. The linear system can then be solved as

$$\vec{G} = -\vec{g}_0(M - I)^{-1}, \quad (16)$$

which is well defined as long as the spectral radius of the matrix M is less than one [18]. The fact that we are considering unfolded self-avoiding walks yields the final condition that the walks must end in one of the first $w + 1$ column states (recall that the convention was made that the column states are labeled in such a way so as to have the first $w + 1$ of them consisting of single horizontal edges), and hence the grand canonical partition function of interest (2) is given by

$$H = \sum_{c=1}^{w+1} G(c) \quad (17)$$

which can be obtained by multiplying the row vector \vec{G} on the right by a column vector consisting of $w + 1$ ones followed by $c_w - (w + 1)$ zeros.

As indicated by (4), for fixed wall interaction parameters \vec{a} and \vec{b} one can then obtain the free energy of the system from the radius of convergence $z_c(H(\vec{a}, \vec{b}, w, z))$ of the grand canonical partition function $H(\vec{a}, \vec{b}, w, z)$. Following arguments as given in [13], the matrix M can be proven to be primitive and hence, by the Perron–Frobenius theorem, it has a unique positive eigenvalue with largest modulus. The radius of convergence can then be obtained from the pole of $(M - I)^{-1}$ with smallest modulus, or equivalently from the zero of $\det(M - I)$ with smallest modulus [13].

One can also obtain the free energy by using the power method [19] on the matrix form of (11), given by

$$\vec{g}_{x+1} = \vec{g}_x M, \quad (18)$$

where $\vec{g}_x = (g_x(1), \dots, g_x(c_w))$. By recursion then

$$\vec{g}_{x+1} = \vec{g}_0 M^x \quad (19)$$

and by considering $\lim_{x \rightarrow \infty} \vec{g}_x$, one has to look for the value of z for which the matrix M has its largest eigenvalue equal to one (otherwise \vec{g}_x vanishes or diverges). Then $\lim_{x \rightarrow \infty} \vec{g}_x$ becomes the left eigenvector of M with eigenvalue one.

4. Results

We are interested in the behavior of the system as a function of the wall interaction parameters \vec{a} and \vec{b} and the width w , in particular, the nature of the forces. In this section we present results for both self-avoiding walks and self-avoiding polygons in the four different models described in the introduction. Section 4.1 presents results for the model with single layers at both walls, section 4.2 discusses the model with a double layer at the top wall, section 4.3 addresses the model with double layers at both walls, and section 4.4 describes results for the model with fully interacting double layers.

4.1. Single layers at both walls

We first consider the case in which the walk interacts with a single layer at each of the confining lines. In this case, the interaction with the confining lines occurs only on direct contact, i.e. when the horizontal edges are at heights $y = 0$ or $y = w$. The interaction at the bottom wall is set to $a_0 = a$, the interaction at the top wall is set to $b_t = b$, and all other wall interactions are

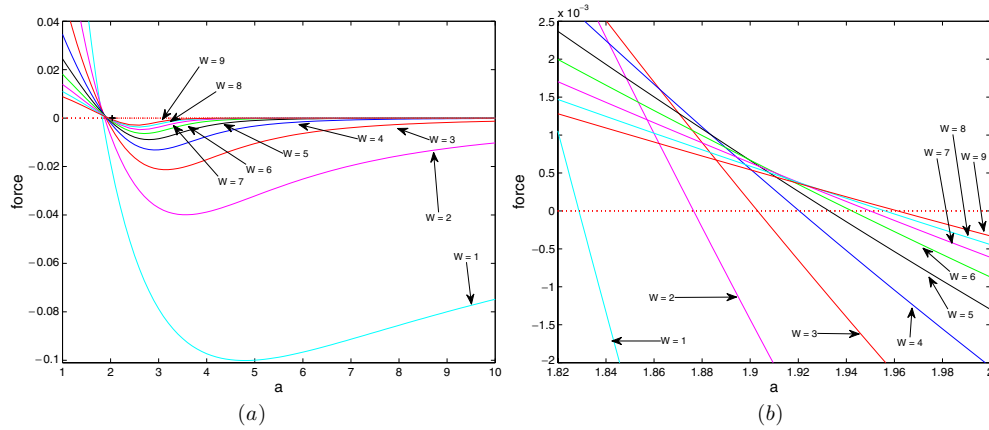


Figure 5. Force for self-avoiding walks in slits of widths $w = 1, \dots, 9$ with single layers at both walls when $a = b$. A positive force corresponds to a repulsive regime and a negative force corresponds to an attractive regime. Sub-figure (b) is the portion of sub-figure (a) around the zero-force crossing point.

turned off by setting $a_{0,1} = a_1 = b_{t-1} = b_{t-1,t} = 1$. The partition function for self-avoiding walks (1) becomes

$$Z_n(\vec{a}, \vec{b}, w) = \sum_{\vec{v}} c_n(\vec{v}, w) a^{v_0} b^{v_w}. \tag{20}$$

The phase diagrams for both Dyck and Motzkin path models were investigated in the large- w regime [6, 8] and several different force regimes were identified: a long-ranged (the force decays as a power law in w) and repulsive regime, a short-ranged (the force decays exponentially in w) and attractive regime, and a short-ranged and repulsive regime. In figures 5 and 6 we observe that the two-dimensional self-avoiding walks also present attractive and repulsive regimes for the slit widths considered here, although we have not determined whether these forces are short-ranged or long-ranged because one needs the asymptotic behavior of the force as the width w diverges.

Figure 5 plots the force as a function of the wall interaction parameter a when $a = b$ for self-avoiding walks in slits of widths $w = 1, \dots, 9$ with single layers at both walls. Note that the force is repulsive (it is positive) for small values of a . As a increases, the force decreases until it becomes an attractive force (it is negative). The force is not a monotonic function, as can be clearly observed in figure 5(a). Even though for large values of a the force is increasing, we found that it stayed below zero as a got larger. That is, we did not locate a second repulsive regime at large values of a . The same behavior was observed in the $a = b$ case in a similar self-avoiding walk model [3] (where the interaction occurs at the vertices, rather than at the edges of the walk), and in the three-dimensional case for short walks [5].

Next, we consider general values of the wall interaction parameters a and b (see figure 6) and obtain similar behavior when one parameter (a or b) is held constant at a value larger than one and the other parameter is increased, that is: the force is repulsive (positive) for small values of the parameter, it decreases until it becomes attractive (negative), and eventually it increases again without becoming repulsive (positive) again. This behavior was conjectured in [4] and observed in similar directed walk (Dyck path and Motzkin path) models [6, 8]. The zero-force curve found in the directed walk models in [6, 8] is independent of the width of the slit. The behavior for self-avoiding walks is different, the location of the zero-force curve

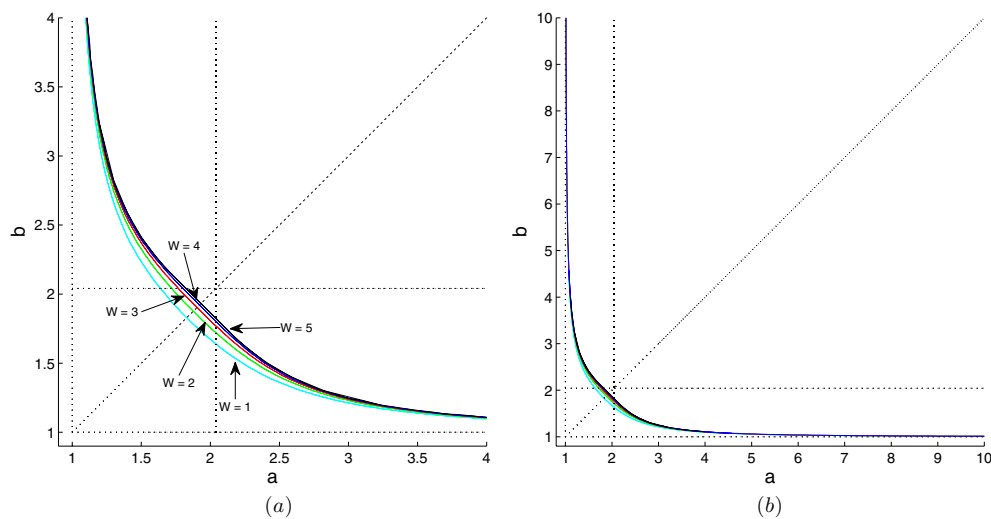


Figure 6. Zero-force curve for self-avoiding walks in slits of widths $w = 1, \dots, 5$ with single layers at both walls. The repulsive region (where the force is positive) is the region south-west of the curves and the attractive region (where the force is negative) is the north-east region. The vertical and horizontal lines around 2.038 indicate the estimated adsorption transition point for self-avoiding walks. The diagonal line is the $a = b$ line. Sub-figure (b) shows that the curves exhibit a vertical asymptote (as $b \rightarrow \infty$) at $a = 1$ and a horizontal asymptote (as $a \rightarrow \infty$) at $b = 1$.

in our model does depend on the width of the slit. Figure 6 plots the zero-force curve for self-avoiding walks in slits of widths $w = 1, \dots, 5$ with single layers at both walls, where the repulsive region (where the force is positive) is the region south-west of the curves and the attractive region (where the force is negative) is the north-east region. The curves never cross one another.

It was shown in [4] that the zero-force curves lay to the right of the vertical line $a = 1$ and above the horizontal line $b = 1$. One can observe in figure 6(b) that the curves exhibit a vertical asymptote (as $b \rightarrow \infty$) at $a = 1$ and a horizontal asymptote (as $a \rightarrow \infty$) at $b = 1$. The vertical and horizontal lines at 2.038 indicate the estimated adsorption transition point for self-avoiding walks [20], and it seems that along the $a = b$ line, the zero-force curves approach the adsorption transition point. This can be observed in figure 7, which plots the zero-force point along the $a = b$ line as a function of $1/w$. The point marked by a star on the vertical axis corresponds to the estimated adsorption transition point for self-avoiding walks: $a \approx 2.038$.

The repulsive and attractive regimes for self-avoiding walks in a slit with single layers at both walls can be explained intuitively because for small wall interaction parameters, there is an entropy loss from the geometrical confinement leading to a repulsive force. However, if one of the wall interaction parameters is large (say a) and the other is small (say b), then conformations of the walk with short excursions but which otherwise stay close to the bottom wall should dominate the partition function and determine the free energy. If the large wall interaction parameter (say a) is fixed and the other parameter (say b) increases, there will be a point where conformations which cross over from one side of the slit to the other begin to contribute significantly to the free energy, and eventually dominate it. In this case the walk will increase its free energy if the confining lines are moved closer together, as the energy

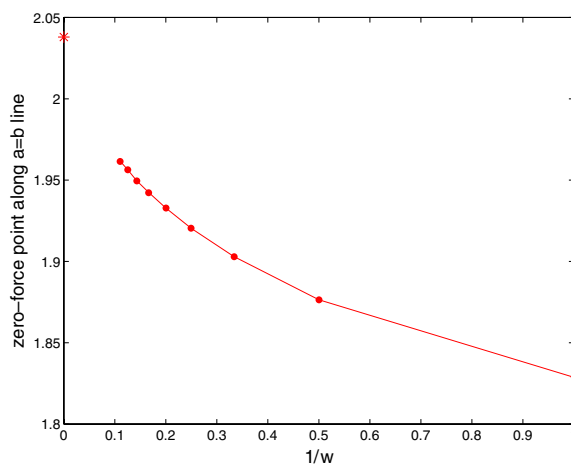


Figure 7. Zero-force point along the $a = b$ line. The point marked by a star on the vertical axis corresponds to the estimated adsorption transition point for self-avoiding walks: $a \approx 2.038$.

increase from visits to both confining lines overcomes the resulting decrease in entropy. Hence the force becomes attractive for large wall interaction parameters.

On the other hand, self-avoiding polygons in a slit with single layers at both walls behave differently. Specifically, as shown next in lemma 2, there are infinitely many values of width w for which the force is never attractive. Intuitively, this is because the polygon is a topological circle so, in the square lattice, the bottom side of the polygon prevents its top side from reaching the bottom wall (and vice versa) to interact with it. Hence, even if the wall interaction parameters are large, keeping the confining lines close together does not increase the free energy. This topological constraint can be overcome with the addition of a second layer of interaction to the walls, as will be described in sections 4.2, 4.3 and 4.4.

Lemma 1. Consider self-avoiding polygons in a slit with single layers at both walls. Then, for any positive width w the free energy difference from increasing the width by a distance of at least w units is non-negative, i.e.

$$\kappa(\vec{a}, \vec{b}, w + i) - \kappa(\vec{a}, \vec{b}, w) \geq 0$$

for integer $i \geq w$.

Proof. Let w be any positive width and let $i \geq w$ be an integer. Take any self-avoiding polygon of length n in a slit of width w with v_0 edges at the bottom wall and v_w edges at the top wall.

Choose the top-most edge among the left-most vertical edges of the polygon (there is always such an edge) and choose the top-most edge among the right-most vertical edges (there is always such an edge). Cut the polygon at the lexicographic top vertices of the two chosen vertical edges to obtain two disjoint self-avoiding walks with the same span in the x -direction. All the visits from the polygon to the top wall of the slit are part of one of the walks (we shall refer to this walk as the *top* walk), and all the visits from the polygon to the bottom wall are part of the other walk (to which we shall refer as the *bottom* walk). This separation, into two disjoint walks, of the top and bottom visits of the polygon does not always occur in higher dimensions. Note that the highest edge of the bottom walk has height $y < w$ and that the lowest edge of the top walk has height $y > 0$.

Now increase the slit width to $w + i$, translate the top walk a distance i units up, and reconnect the two disjoint walks with i vertical edges on each side. The translation of the top walk by a distance $i \geq w$ serves two purposes. First, it ensures that the lowest edge of the top walk has height $y > w$, which is above the highest edge of the bottom walk. Hence, there is no overlapping between the walks and the resulting object is a self-avoiding polygon of length $n + 2i$ in a slit of width $w + i$. Second, all edges that were previously at a distance w from the bottom wall are now at a distance $w + i$ so that all the edges that were originally at the top wall (in the slit of width w) are still at the top wall (now in the slit of width $w + i$). The bottom walk was not translated so all the edges that were previously at the bottom wall are still there. Therefore, the resulting self-avoiding polygon also has v_0 edges at the bottom wall and v_w edges at the top wall.

For each distinct self-avoiding polygon of length n in a slit of width w , this procedure creates a unique self-avoiding polygon of length $n + 2i$ in a slit of width $w + i$ and no two self-avoiding polygons in a slit of width w yield the same self-avoiding polygon in a slit of width $w + i$. Therefore,

$$p_n(w, v_0, v_w) \leq p_{n+2i}(w + i, v_0, v_w), \tag{21}$$

where $p_n(w, v_0, v_w)$ is the number of polygons of length n in a slit of width w with v_0 horizontal edges at the bottom wall and v_w horizontal edges at the top wall. Then, multiplying by $a^{v_0}b^{v_w}$, summing over v_0, v_w , taking logarithms, dividing by n and taking the limit as $n \rightarrow \infty$ yields:

$$\lim_{n \rightarrow \infty} n^{-1} \log \left(\sum_{v_0, v_w} p_n(w, v_0, v_w) a^{v_0} b^{v_w} \right) \leq \lim_{n \rightarrow \infty} n^{-1} \log \left(\sum_{v_0, v_w} p_{n+2i}(w + i, v_0, v_w) a^{v_0} b^{v_w} \right) \tag{22}$$

$$\kappa(a, b, w) \leq \kappa(a, b, w + i). \tag{23}$$

The existence of the limits in (22) follows *mutatis mutandis* from [4, 21]. Then

$$0 \leq \kappa(a, b, w + i) - \kappa(a, b, w). \tag{24}$$

Therefore, for any positive width w the free energy difference from increasing the width by a distance of at least w units is non-negative, and the lemma is proved. \square

Lemma 2. *There are infinitely many values of width w for which the force for self-avoiding polygons in a slit of width w with single layers at both walls is always non-attractive (non-negative).*

Proof. Let w be any positive width, take equation (24) from lemma 1 with $i = w$ and expand it as a telescopic sum to obtain

$$0 \leq \kappa(a, b, 2w) - \kappa(a, b, w) = \sum_{m=0}^{w-1} (\kappa(a, b, w + m + 1) - \kappa(a, b, w + m)) = \sum_{m=0}^{w-1} f_{w+m}(\vec{a}, \vec{b}). \tag{25}$$

The right-hand side of (25) is non-negative, thus at least one of the terms $f(\vec{a}, \vec{b}, i) := \kappa(a, b, i + 1) - \kappa(a, b, i)$ for $i = w, \dots, 2w - 1$ has to be non-negative. The width w was chosen arbitrarily, so that for each positive width w there is at least one other width $\hat{w} \in \{w, w + 1, \dots, 2w - 1\}$ with $f(\vec{a}, \vec{b}, \hat{w}) \geq 0$. Therefore, there are infinitely many values of width w for which the force $f(\vec{a}, \vec{b}, \hat{w})$ for self-avoiding polygons in a slit of width w with single layers at both walls is always non-negative, and the lemma is proved. \square

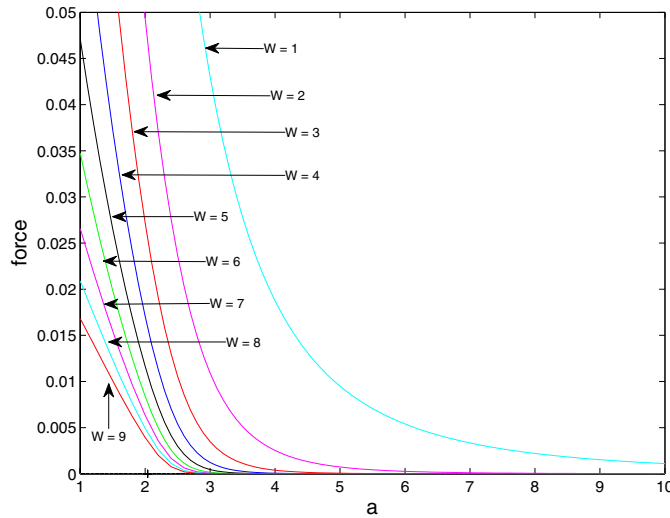


Figure 8. Force along the $a = b$ line for self-avoiding polygons in slits of widths $w = 1, \dots, 9$ with single layers at both walls. A positive force corresponds to a repulsive regime. The observation that the forces are always positive is consistent with lemma 2.

Figure 8 plots the force along the $a = b$ line for self-avoiding polygons in slits of widths $w = 1, \dots, 9$ with single layers at both walls. The observation that the forces are always positive is consistent with lemma 2.

4.2. Double layer at the top wall

We proved in section 4.1 that there is no attractive regime for infinitely many slit widths for self-avoiding polygon models with single layers at both walls, and we saw that the widths $w = 1, 2, \dots, 9$ are example widths for which this holds. We argued that this was due to the fact that the polygon is a topological circle so the top side of the polygon prevents the bottom side from being able to reach the top wall (and vice versa) to increase its free energy. In this section we examine a model with a double layer at the top wall so that a horizontal edge in the polygon or walk interacts with the top wall if it is at height $y = w$ or at height $y = w - 1$. This is to counteract the shielding effect of the polygon so that although the top side of the polygon still prevents the bottom side from interacting with the top layer of the top wall, now the bottom side can interact with the second layer of the top wall. The interaction with the top wall then is modeled by setting $b_{t-1} = b_t = b$, while the interaction at the bottom wall is set to $a_0 = a$, and all other wall interactions are turned off by setting $a_{0,1} = a_1 = b_{t-1,t} = 1$. The partition function (1) becomes

$$Z_n(\vec{a}, \vec{b}, w) = \sum_{\vec{v}} c_n(\vec{v}, w) a^{v_0} b^{v_{w-1} + v_w}. \tag{26}$$

In this model, both self-avoiding walks and self-avoiding polygons exhibit attractive and repulsive regimes. Figure 9 plots the zero-force curves for self-avoiding walks in slits of widths $w = 2, \dots, 5$ with a double layer at the top wall. The curves do not cross one another and in this model the curves are not symmetric about the $a = b$ line. The curve for width $w = 1$ is a degenerate case and is not plotted in the figure. Observe in figure 9(b) that the

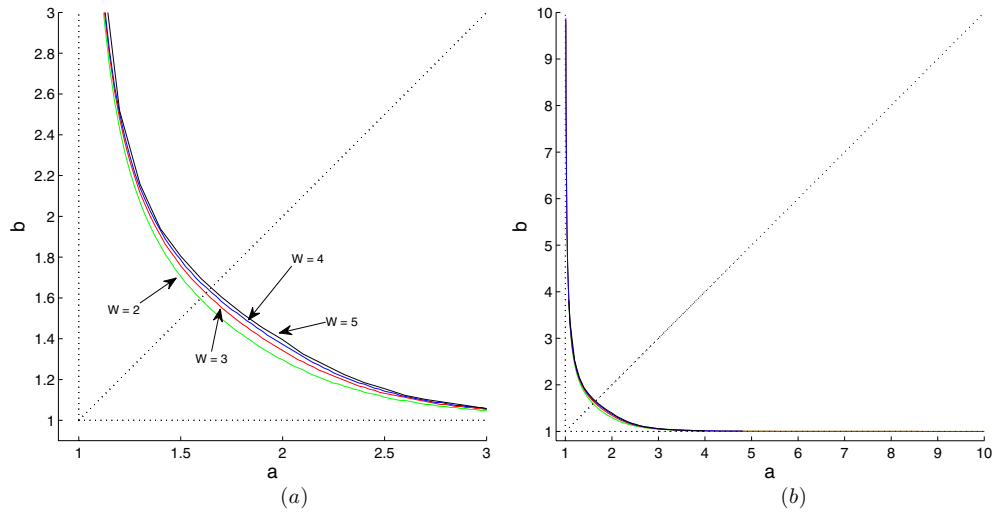


Figure 9. Zero-force curve for self-avoiding walks in slits of widths $w = 2, \dots, 5$ with a double layer at the top wall. The repulsive region (where the force is positive) is the region south-west of the curves and the attractive region (where the force is negative) is the north-east region. The diagonal line is the $a = b$ line. Sub-figure (b) shows that the curves exhibit a vertical asymptote (as $b \rightarrow \infty$) at $a = 1$ and a horizontal asymptote (as $a \rightarrow \infty$) at $b = 1$.

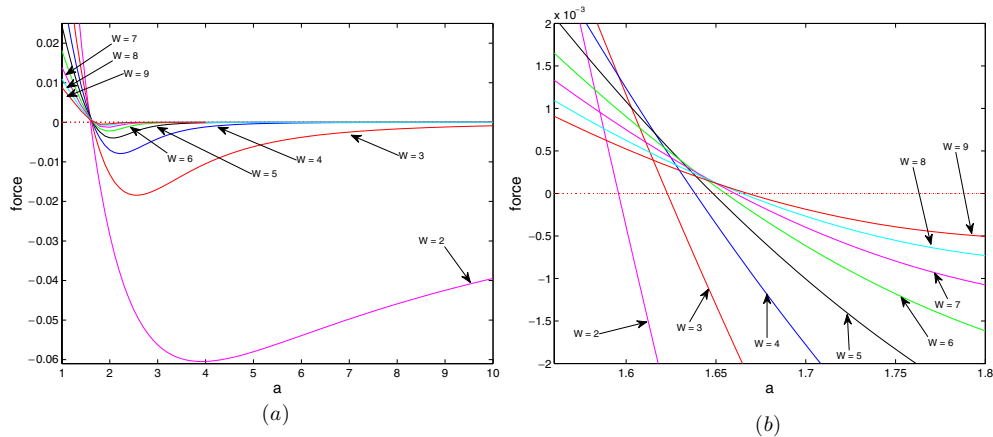


Figure 10. Force along the $a = b$ line for self-avoiding walks in a slit of width $w = 2, \dots, 9$ with a double layer at the top wall. A positive force corresponds to a repulsive regime and a negative force corresponds to an attractive regime. Sub-figure (b) is the portion of sub-figure (a) around the zero-force crossing point.

curves exhibit a vertical asymptote (as $b \rightarrow \infty$) at $a = 1$ and a horizontal asymptote (as $a \rightarrow \infty$) at $b = 1$.

Figure 10 plots the force along the $a = b$ line in the phase diagram for self-avoiding walks in slits of widths $w = 2, \dots, 9$ with a double layer at the top wall. The force is repulsive (positive) for small values of the wall interaction parameter a but it decreases until it becomes attractive (negative). For increasingly larger values of a the force goes through a minimum

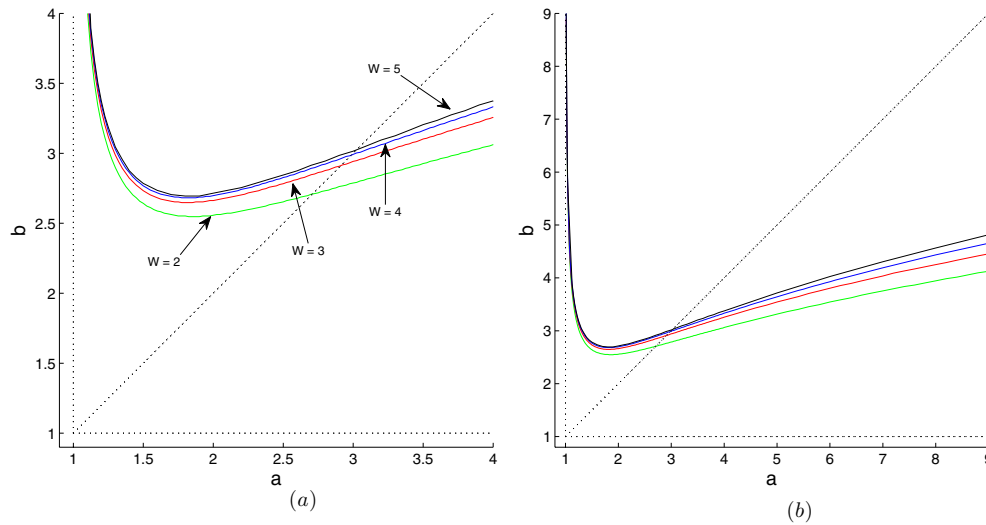


Figure 11. Zero-force curve for self-avoiding polygons in slits of widths $w = 2, \dots, 5$ with a double layer at the top wall. The repulsive region (where the force is positive) is the region south-west of the curves and the attractive region (where the force is negative) is the north-east region. The diagonal line is the $a = b$ line. Sub-figure (b) shows that the curves exhibit a vertical asymptote (as $b \rightarrow \infty$) at $a = 1$ and that there is re-entrant behavior for large b as a increases.

(where the attraction is maximal) and then increases to less negative values. However, the force remains negative (and attractive) and seems to approach a zero-force as a increases without bound.

Figure 11 plots the zero-force curve for self-avoiding polygons in slits of widths $w = 2, \dots, 5$ with a double layer at the top wall. These curves are not symmetric about the $a = b$ line. By looking at a wall interaction parameter $b = 3$, say, and considering increasing values of the wall interaction parameter a the force goes from being repulsive to being attractive and then back to being repulsive; this is referred to as a *re-entrant* behavior. It appears that for any sufficiently large value of b , a re-entrant behavior is observed as a increases. The curves exhibit a vertical asymptote (as $b \rightarrow \infty$) at $a = 1$. The curve for width $w = 1$ is not plotted because it is a degenerate case.

Figure 12 plots the force along the $a = b$ line for self-avoiding polygons in slits of widths $w = 2, \dots, 9$ with a double layer at the top wall. While the force is repulsive for small values of the wall interaction parameters a and b , it decreases with increasing values of the parameters and becomes attractive. As pointed out in the beginning of this subsection, in this double layer model the bottom side of the polygon can cross over the slit to interact with the top wall. These conformations of the polygon make a dominating contribution to the free energy for large values of a and b , and thus creating an attractive regime—in contrast to the single layer model where screening prevents the formation of an attractive regime.

4.3. Double layers at both walls

This section presents a model with double layers at both walls. Interactions between the polymer and the walls occur in this case whenever horizontal edges of the walk or polygon are at heights $y \in \{0, 1, w - 1, w\}$. We model interactions with the bottom wall by setting

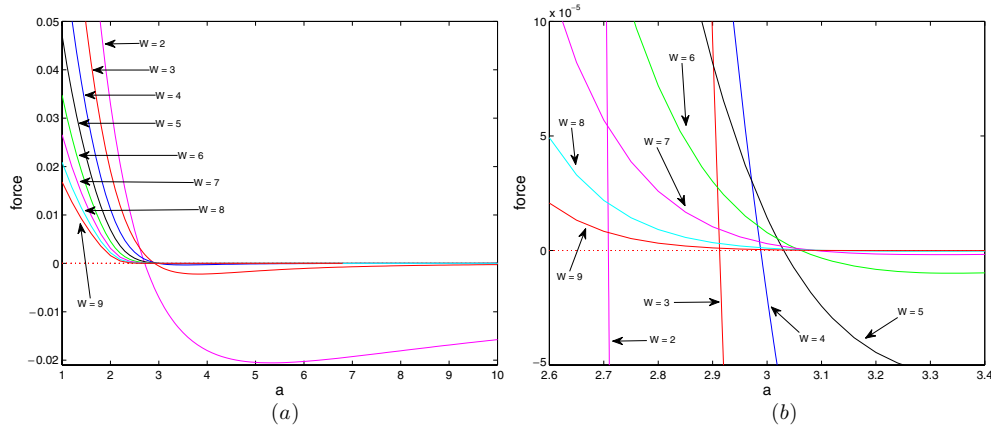


Figure 12. Force along the $a = b$ line for self-avoiding polygons in slits of widths $w = 2, \dots, 9$ with a double layer at the top wall. A positive force corresponds to a repulsive regime and a negative force corresponds to an attractive regime. Sub-figure (b) is the portion of sub-figure (a) around the zero-force crossing point.

$a_0 = a_1 = a$ and with the top wall by setting $b_{t-1} = b_t = b$. The remaining wall interactions are turned off by choosing $a_{0,1} = b_{t-1,t} = 1$. In this model the partition function (1) is

$$Z_n(\vec{a}, \vec{b}, w) = \sum_{\vec{v}} c_n(\vec{v}, w) a^{v_0+v_1} b^{v_{w-1}+v_w}. \quad (27)$$

Figure 13 plots the zero-force curve for self-avoiding walks in slits of widths $w = 2, \dots, 5$ with double layers at both walls. The curves are symmetric about the $a = b$ line. One can observe in figure 13(b) that the curves exhibit a vertical asymptote (as $b \rightarrow \infty$) at $a = 1$ and a horizontal asymptote (as $a \rightarrow \infty$) at $b = 1$.

Figure 14 plots the force along the $a = b$ line for self-avoiding walks in slits of widths $w = 3, \dots, 9$ with a double layer at both walls. The curves for widths $w = 1, 2$ are not plotted because they are degenerate.

Figure 15 plots the zero-force curve for self-avoiding polygons in slits of widths $w = 3, \dots, 6$ with double layers at both walls. The curves are symmetric about the $a = b$ line, and the curves for widths $w = 1, 2$ are not plotted due to their degeneracy. Observe in figure 15(b) that the curves exhibit a vertical asymptote (as $b \rightarrow \infty$) at $a = 1$ and a horizontal asymptote (as $a \rightarrow \infty$) at $b = 1$.

Figure 16 plots the force along the $a = b$ line for self-avoiding polygons in slits of widths $w = 3, \dots, 9$ with double layers at both walls.

It is not clear from our results for this model whether or not the zero-force point along the line $a = b$ diverges as $w \rightarrow \infty$. This remains an open question in this model.

4.4. The fully interacting double layer model

Finally, this section presents a model where all the wall interactions in the partition function (1) are included, but with the restriction that all interactions near the bottom wall are equal, i.e. $a_0 = a_{0,1} = a_1 = a$, and all interactions near the top wall are equal, i.e. $b_{t-1} = b_{t-1,t} = b_t = b$. The partition function (1) becomes

$$Z_n(\vec{a}, \vec{b}, w) = \sum_{\vec{v}} p_n(\vec{v}, w) a^{v_0+v_{0,1}+v_1} b^{v_{w-1}+v_{w-1,w}+v_w}. \quad (28)$$

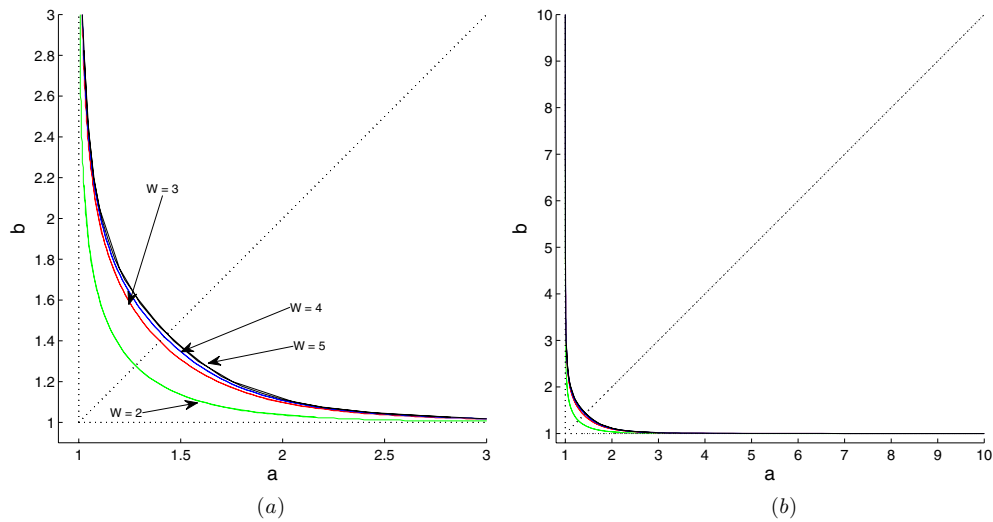


Figure 13. Zero-force curve for self-avoiding walks in slits of widths $w = 2, \dots, 5$ with double layers at both walls. The repulsive region (where the force is positive) is the region south-west of the curves and the attractive region (where the force is negative) is the north-east region. The diagonal line is the $a = b$ line. Sub-figure (b) shows that the curves exhibit a vertical asymptote (as $b \rightarrow \infty$) at $a = 1$ and a horizontal asymptote (as $a \rightarrow \infty$) at $b = 1$.

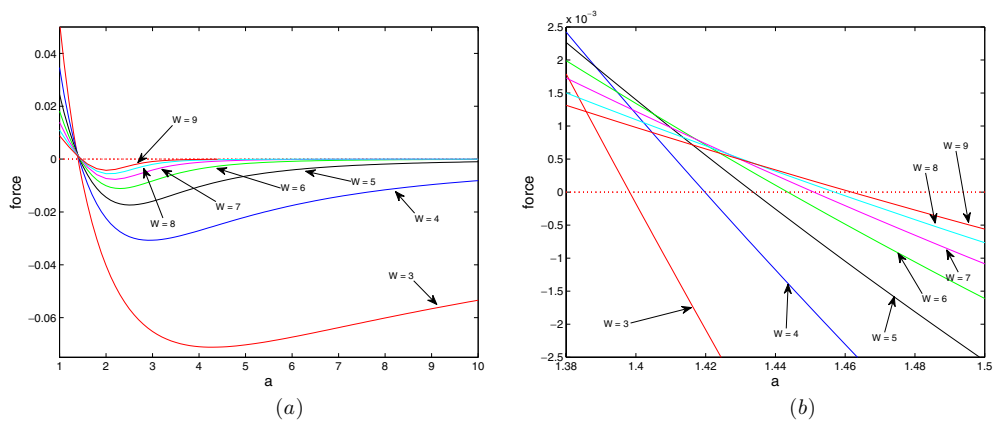


Figure 14. Force along the $a = b$ line for self-avoiding walks in slits of widths $w = 3, \dots, 9$ with double layers at both walls. A positive force corresponds to a repulsive regime and a negative force corresponds to an attractive regime. Sub-figure (b) is the portion of sub-figure (a) around the zero-force crossing point.

Figure 17 plots the zero-force curve for self-avoiding polygons in slits of widths $w = 3, \dots, 7$ with fully interacting double layers at both walls. The curves are symmetric about the $a = b$ line. There is a re-entrant behavior in some regions of the phase diagram and the curves exhibit a vertical asymptote (as $b \rightarrow \infty$) at $a = 1$ and a horizontal asymptote (as $a \rightarrow \infty$) at $b = 1$. The curves for widths $w = 1, 2$ are not plotted because they are degenerate cases.

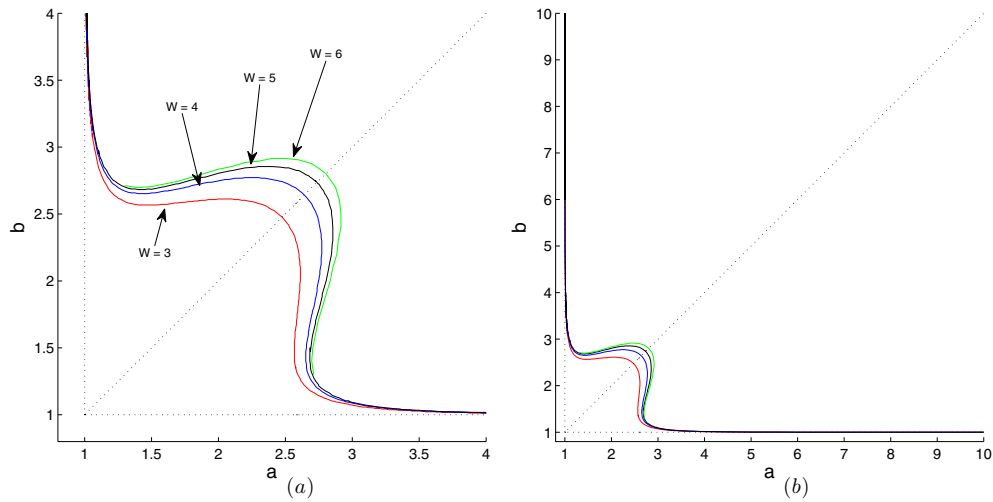


Figure 15. Zero-force curve for self-avoiding polygons in slits of widths $w = 3, \dots, 6$ with double layers at both walls. The repulsive region (where the force is positive) is the region south-west of the curves and the attractive region (where the force is negative) is the north-east region. The diagonal line is the $a = b$ line. Sub-figure (b) shows that the curves exhibit a vertical asymptote (as $b \rightarrow \infty$) at $a = 1$ and a horizontal asymptote (as $a \rightarrow \infty$) at $b = 1$.

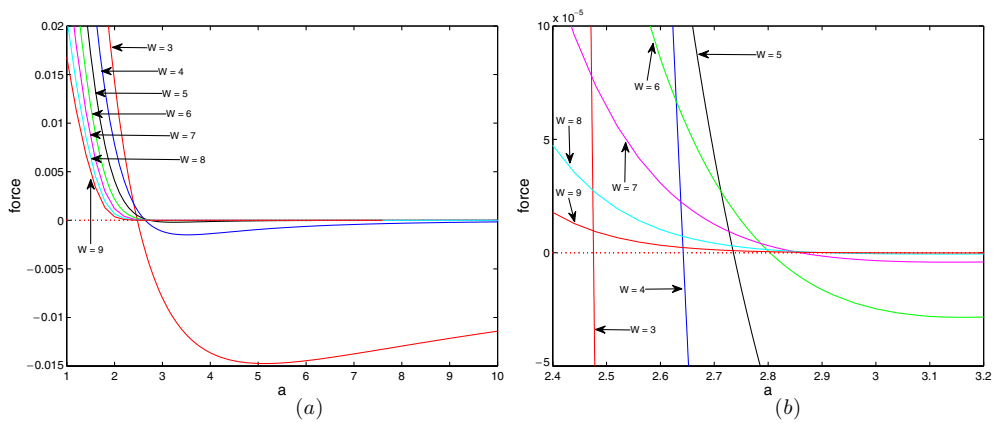


Figure 16. Force along the $a = b$ line for self-avoiding polygons in slits of widths $w = 3, \dots, 9$ with double layers at both walls. A positive force corresponds to a repulsive regime and a negative force corresponds to an attractive regime. Sub-figure (b) is the portion of sub-figure (a) around the zero-force crossing point.

Figure 18 plots the force along the $a = b$ line for self-avoiding polygons in slits of widths $w = 3, \dots, 7$ with fully interacting double layers at both walls. The curves for widths $w = 1, 2$ are not plotted due to their degeneracy.

It is not clear from our results for this model whether or not the zero-force point along the line $a = b$ diverges as $w \rightarrow \infty$. This remains an open question in this model, as well as in the self-avoiding polygon model with double layers at both walls (figure 15). In contrast,

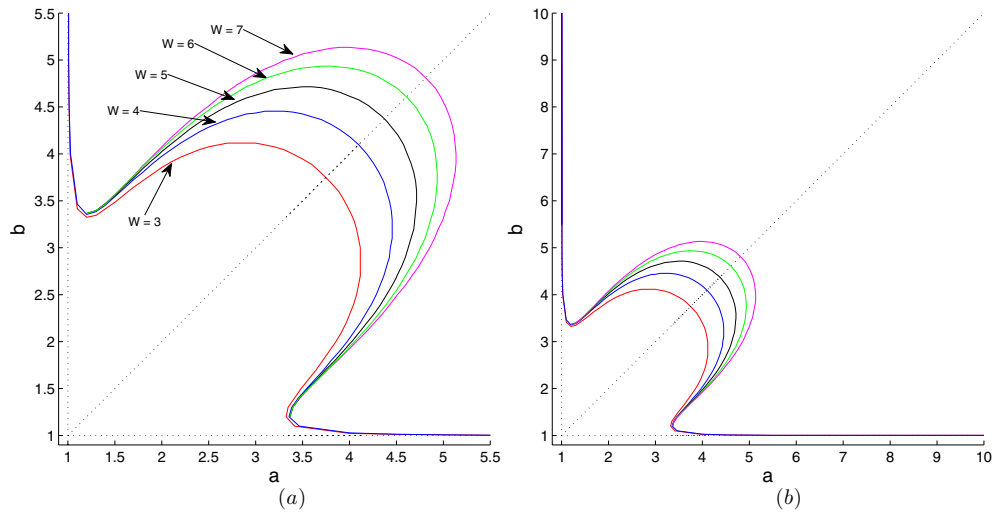


Figure 17. Zero-force curve for self-avoiding polygons in slits of widths $w = 3, \dots, 7$ with fully interacting double layers at both walls. The repulsive region (where the force is positive) is the region south-west of the curves and the attractive region (where the force is negative) is the north-east region. The diagonal line is the $a = b$ line. Sub-figure (b) shows that the curves exhibit a vertical asymptote (as $b \rightarrow \infty$) at $a = 1$ and a horizontal asymptote (as $a \rightarrow \infty$) at $b = 1$.

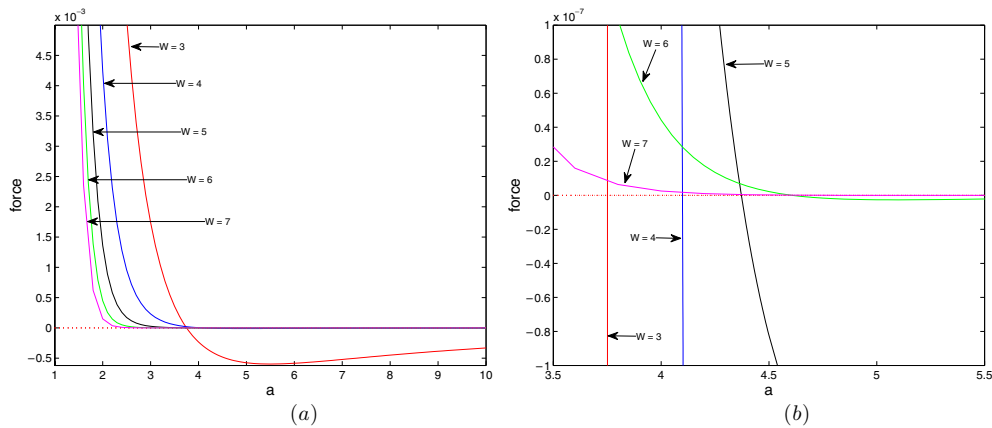


Figure 18. Force along the $a = b$ line for self-avoiding polygons in a slit of width $w = 3, \dots, 7$ with fully interacting double layers at both walls. A positive force corresponds to a repulsive regime and a negative force corresponds to an attractive regime. Sub-figure (b) is the portion of sub-figure (a) around the zero-force crossing point.

the self-avoiding walks do not seem to diverge (see figures 6, 9 and 13). In particular, in the single-layer case (figure 6), it seems to converge to the adsorption transition point.

5. Conclusions

We considered several models of walks and polygons confined to a two-dimensional slit in the square lattice interacting with the walls of the slit. Our main approach was based on

transfer-matrix calculations. This limited our models to slits of width at most 10 in most cases, and width 8 in the model with fully interacting double layers. Larger values of w appear to be beyond the scope of available computational resources.

Differences in the force diagrams were seen for polygons and walks in the model with single layers. This is, for example, explicitly seen in figures 5 and 8, where one notes the absence of an attractive regime in the polygon model (figure 8), while an attractive regime is clearly present in the walk model (figure 5). We show in lemma 2 that there are infinitely many values of width w where there is no attractive regime in the polygon model. While we expect that this result can be extended to all values of w , we have not proved this. In this context, the transfer matrix results demonstrate rigorously the existence of an attractive regime in the walk model for the values of w considered.

In the other models we saw attractive and repulsive regimes for both the walk and the polygon models. We plotted zero-force curves for each of the models in figures 9, 11, 13, 15 and 17. In the models with double layers the zero-force curve is convex in the ab -plane for walk models (figures 9 and 13), as well as for polygons when there is a single layer at one wall and a double layer at the other (figure 11). A more interesting result is obtained for polygons with double layers at both walls and with fully interacting double layers (figures 15 and 17, respectively). In these cases, the zero-force curve is not convex, and the shape of this curve for large w is an open question.

Acknowledgments

The authors acknowledge support from the Discovery Grants Program of NSERC of Canada.

References

- [1] de Gennes P G 1979 *Scaling Concepts in Polymer Physics* (Ithaca, NY: Cornell University Press)
- [2] DiMarzio E A and Rubin R J 1971 *J. Chem. Phys.* **55** 4318–36
- [3] Stilck J F and Machado K D 1998 *Eur. Phys. J. B* **5** 899–904
- [4] Janse van Rensburg E J, Orlandini E and Whittington S G 2006 *J. Phys. A: Math. Gen.* **39** 13869–902
- [5] Janse van Rensburg E J, Orlandini E, Owczarek A L, Rechnitzer A and Whittington S G 2005 *J. Phys. A: Math. Gen.* **38** L823–8
- [6] Brak R, Owczarek A L, Rechnitzer A and Whittington S G 2005 *J. Phys. A: Math. Gen.* **38** 4309–25
- [7] Owczarek A L, Prellberg T and Rechnitzer A 2008 *J. Phys. A: Math. Theor.* **41** 035002:1–16
- [8] Brak R, Iliev G K, Rechnitzer A and Whittington S G 2007 *J. Phys. A: Math. Theor.* **40** 4415–37
- [9] Wall F T, Seitz W A and Chin J C 1977 *J. Chem. Phys.* **67** 434–8
- [10] Wall F T, Mandel F and Chin J C 1976 *J. Chem. Phys.* **65** 2231–4
- [11] Wall F T, Seitz W A, Chin J C and de Gennes P G 1978 *Proc. Natl Acad. Sci.* **75** 2069–70
- [12] Klein D J 1980 *J. Stat. Phys.* **23** 561–86
- [13] Alm S E and Janson S 1990 *Commun. Stat. Stoch. Models.* **6** 169–212
- [14] Hammersley J M and Whittington S G 1985 *J. Phys. A: Math. Gen.* **18** 101–11
- [15] Stanley R 1986 *Enumerative Combinatorics* vol I (Monterey: Wadsworth & Brooks/Cole)
- [16] Hammersley J M and Welsh D J A 1962 *Q. J. Math. Oxford Ser.* **2** 108–10
- [17] Sloane N J A 2007 The on-line encyclopedia of integer sequences, published electronically at www.research.att.com/~njas/sequences/A000108
- [18] Lebedev V I 1997 *An Introduction to Functional Analysis in Computational Mathematics* (Boston, MA: Birkhäuser)
- [19] Saad Y 1992 *Numerical Methods For Large Eigenvalue Problems* (Toronto, Ontario: Halsted Press)
- [20] Grassberger P and Hegger R 1995 *Phys. Rev. E* **51** 2674–6
- [21] Soteros C E and Whittington S G 1988 *J. Phys. A: Math. Gen.* **21** L857–L861